SCIENCE CHINA
Information Sciences

• **Supplementary File** •

Adaptive synchronization control of uncertain multiple USVs with prescribed performance and preserved connectivity

Shude HE[1], Shi-Lu DAI[1*] & Chao DONG[2]

[1]*School of Automation Science and Engineering, South China University of Technology, Guangzhou* 510641*, China;*
[2]*South China Sea Marine Survey and Technology Center, Guangzhou* 510300*, China*

Appendix A Proof of Theorem 1

To facilitate the proof of Theorem 1, we present the following two lemmas.

Lemma 1. Consider the directed graph $\bar{\mathcal{G}}$ with a directed spanning tree. If $|\frac{p_{ij,l}}{\rho_{ij,l}}| < 1$ and $p_{ij,l} \neq 0$, then we have

$$\|\boldsymbol{\eta} - \bar{\boldsymbol{\eta}}_0 + \boldsymbol{c}\| \leqslant \frac{\|\boldsymbol{s}\|}{\sigma_{\min}(\boldsymbol{L}_N + \boldsymbol{B}_L)} \tag{A1}$$

with $\boldsymbol{\eta} = [\boldsymbol{\eta}_1^T, \boldsymbol{\eta}_2^T, \ldots, \boldsymbol{\eta}_N^T]^T$, $\bar{\boldsymbol{\eta}}_0 = [\boldsymbol{\eta}_0, \ldots, \boldsymbol{\eta}_0]^T \in \Re^{3N}$, $\boldsymbol{c} = [\boldsymbol{c}_1^T, \boldsymbol{c}_2^T, \ldots, \boldsymbol{c}_N^T]^T$, $\boldsymbol{s} = [\boldsymbol{s}_1^T, \boldsymbol{s}_2^T, \ldots, \boldsymbol{s}_N^T]^T$, $\boldsymbol{L}_N = [\boldsymbol{l}_{ij}] \in \Re^{3N\times 3N}$, $i = 1, \ldots, N$, $j = 1, \ldots, N$,

$$\boldsymbol{l}_{ij} = \begin{cases} \sum\limits_{j=1, j\neq i}^{N} a_{ij}\boldsymbol{\kappa}_{ij}\boldsymbol{\rho}_{ij}^{-1}, & i = j \\ -a_{ij}\boldsymbol{\kappa}_{ij}\boldsymbol{\rho}_{ij}^{-1}, & i \neq j, \end{cases} \tag{A2}$$

$\boldsymbol{\rho}_{ij} = \mathrm{diag}[\rho_{ij,1}, \rho_{ij,2}, \rho_{ij,3}]$, $\boldsymbol{\kappa}_{ij} = \mathrm{diag}[\kappa_{ij,1}, \kappa_{ij,2}, \kappa_{ij,3}]$,

$$\kappa_{ij,l} = 4|\frac{p_{ij,l}}{\rho_{ij,l}}|(1 + \frac{1}{3}(\frac{p_{ij,l}}{\rho_{ij,l}})^2 + \frac{1}{5}(\frac{p_{ij,l}}{\rho_{ij,l}})^4 + ...)^2, \ l = 1, 2, 3 \tag{A3}$$

and $\boldsymbol{B}_L = \mathrm{diag}[a_{10}\boldsymbol{\kappa}_{10}\boldsymbol{\rho}_{10}^{-1}, a_{20}\boldsymbol{\kappa}_{20}\boldsymbol{\rho}_{20}^{-1}, \ldots, a_{N0}\boldsymbol{\kappa}_{N0}\boldsymbol{\rho}_{N0}^{-1}] \in \Re^{3N\times 3N}$, $\boldsymbol{\rho}_{i0} = \mathrm{diag}[\rho_{i0,1}, \rho_{i0,2}, \rho_{i0,3}]$, $\boldsymbol{\kappa}_{i0} = \mathrm{diag}[\kappa_{i0,1}, \kappa_{i0,2}, \kappa_{i0,3}]$, $\kappa_{i0,l} = 4|\frac{p_{i0,l}}{\rho_{i0,l}}|(1 + \frac{1}{3}(\frac{p_{i0,l}}{\rho_{i0,l}})^2 + \frac{1}{5}(\frac{p_{i0,l}}{\rho_{i0,l}})^4 + ...)^2$, $l = 1, 2, 3$. The term $\sigma_{\min}(\boldsymbol{L}_N + \boldsymbol{B}_L)$ in (A1) is the minimum singular value of the matrix $\boldsymbol{L}_N + \boldsymbol{B}_L$.

Proof: From (A3), if $|\frac{p_{ij,l}}{\rho_{ij,l}}| < 1$ holds, then we have the following Taylor series expansion:

$$e_{ij,l} = \ln\frac{1 + \frac{p_{ij,l}}{\rho_{ij,l}}}{1 - \frac{p_{ij,l}}{\rho_{ij,l}}} = 2(\frac{p_{ij,l}}{\rho_{ij,l}})(1 + \frac{1}{3}(\frac{p_{ij,l}}{\rho_{ij,l}})^2 + \frac{1}{5}(\frac{p_{ij,l}}{\rho_{ij,l}})^4 + ...).$$

Using (6), we have

$$\begin{aligned} s_{i,l} &= \sum_{j=1}^{N} a_{ij}[2(\frac{p_{ij,l}}{\rho_{ij,l}})(1 + \frac{1}{3}(\frac{p_{ij,l}}{\rho_{ij,l}})^2 + \frac{1}{5}(\frac{p_{ij,l}}{\rho_{ij,l}})^4 + ...)]^2 + a_{i0}[2(\frac{p_{i0,l}}{\rho_{i0,l}})(1 + \frac{1}{3}(\frac{p_{i0,l}}{\rho_{i0,l}})^2 + \frac{1}{5}(\frac{p_{i0,l}}{\rho_{i0,l}})^4 + ...)]^2 \\ &\geqslant \sum_{j=1}^{N} 4a_{ij}(\frac{p_{ij,l}}{\rho_{ij,l}})|\frac{p_{ij,l}}{\rho_{ij,l}}|(1 + \frac{1}{3}(\frac{p_{ij,l}}{\rho_{ij,l}})^2 + \frac{1}{5}(\frac{p_{ij,l}}{\rho_{ij,l}})^4 + ...)^2 + 4a_{i0}(\frac{p_{i0,l}}{\rho_{i0,l}})|\frac{p_{i0,l}}{\rho_{i0,l}}|(1 + \frac{1}{3}(\frac{p_{i0,l}}{\rho_{i0,l}})^2 + \frac{1}{5}(\frac{p_{ij,l}}{\rho_{ij,l}})^4 + ...)^2 \\ &\geqslant \sum_{j=1}^{N} a_{ij}\kappa_{ij,l}(\frac{p_{ij,l}}{\rho_{ij,l}}) + a_{i0}\kappa_{i0,l}(\frac{p_{i0,l}}{\rho_{i0,l}}) \end{aligned}$$

where $\kappa_{ij,l}$ is defined in (A3). Subsequently, the overall error vector $\boldsymbol{s} = [\boldsymbol{s}_1, \boldsymbol{s}_2, \ldots, \boldsymbol{s}_N]^T$ is described by

$$\begin{pmatrix} \boldsymbol{s}_1 \\ \vdots \\ \boldsymbol{s}_N \end{pmatrix} \geqslant \begin{pmatrix} \sum_{j=1}^{N} a_{1j}\boldsymbol{\kappa}_{1j}\boldsymbol{\rho}_{1j}^{-1}\boldsymbol{p}_{1j} \\ \vdots \\ \sum_{j=1}^{N} a_{Nj}\boldsymbol{\kappa}_{Nj}\boldsymbol{\rho}_{Nj}^{-1}\boldsymbol{p}_{N,j} \end{pmatrix} + \begin{pmatrix} a_{10}\boldsymbol{k}_{10}\boldsymbol{\rho}_{10}^{-1}\boldsymbol{p}_{10} \\ \vdots \\ a_{N0}\boldsymbol{k}_{N0}\boldsymbol{\rho}_{N0}^{-1}\boldsymbol{p}_{10} \end{pmatrix}$$

* Corresponding author (email: audaisl@scut.edu.cn)

$$
\begin{aligned}
&= \operatorname{diag}(\sum_{j=1}^{N} a_{1j}\boldsymbol{\kappa}_{1j}\boldsymbol{\rho}_{1j}^{-1},\ldots,\sum_{j=1}^{N} a_{Nj}\boldsymbol{\kappa}_{Nj}\boldsymbol{\rho}_{Nj}^{-1})\boldsymbol{\eta} + \operatorname{diag}(a_{10}\boldsymbol{\kappa}_{10}\boldsymbol{\rho}_{10}^{-1},\ldots,a_{N0}\boldsymbol{\kappa}_{N0}\boldsymbol{\rho}_{N0}^{-1})(\boldsymbol{\eta}-\bar{\boldsymbol{\eta}}_0)\\
&\quad + \begin{pmatrix} -a_{11}\boldsymbol{\kappa}_{11}\boldsymbol{\rho}_{11}^{-1} & \cdots & -a_{1N}\boldsymbol{\kappa}_{1N}\boldsymbol{\rho}_{1N}^{-1} \\ \vdots & \ddots & \vdots \\ -a_{N1}\boldsymbol{\kappa}_{N1}\boldsymbol{\rho}_{N1}^{-1} & \cdots & -a_{NN}\boldsymbol{\kappa}_{NN}\boldsymbol{\rho}_{NN}^{-1} \end{pmatrix}\boldsymbol{\eta} + \begin{pmatrix} \sum_{j=0}^{N} a_{1j}\boldsymbol{\kappa}_{1j}\boldsymbol{\rho}_{1j}^{-1}\boldsymbol{c}_{1j} \\ \vdots \\ \sum_{j=0}^{N} a_{Nj}\boldsymbol{\kappa}_{Nj}\boldsymbol{\rho}_{Nj}^{-1}\boldsymbol{c}_{Nj} \end{pmatrix}\\
&= \boldsymbol{L}_N\boldsymbol{\eta} + \boldsymbol{B}_L(\boldsymbol{\eta}-\bar{\boldsymbol{\eta}}_0) + \begin{pmatrix} \sum_{j=0}^{N} a_{1j}\boldsymbol{\kappa}_{1j}\boldsymbol{\rho}_{1j}^{-1}\boldsymbol{c}_{1j} \\ \vdots \\ \sum_{j=0}^{N} a_{Nj}\boldsymbol{\kappa}_{Nj}\boldsymbol{\rho}_{Nj}^{-1}\boldsymbol{c}_{Nj} \end{pmatrix}.
\end{aligned}
$$

Notice that $\boldsymbol{L}_N\bar{\boldsymbol{\eta}}_0 = 0$ and

$$
(\boldsymbol{L}_N + \boldsymbol{B}_L)\boldsymbol{c} = \begin{pmatrix} \sum_{j=0}^{N} a_{1j}\boldsymbol{\kappa}_{1j}\boldsymbol{\rho}_{1j}^{-1}\boldsymbol{c}_{1j} \\ \vdots \\ \sum_{j=0}^{N} a_{Nj}\boldsymbol{\kappa}_{Nj}\boldsymbol{\rho}_{Nj}^{-1}\boldsymbol{c}_{Nj} \end{pmatrix}.
$$

Then, we have

$$
\boldsymbol{s} = \boldsymbol{L}_N\boldsymbol{\eta} - \boldsymbol{L}_N\bar{\boldsymbol{\eta}}_0 + \boldsymbol{B}_L(\boldsymbol{\eta}-\bar{\boldsymbol{\eta}}_0) + (\boldsymbol{L}_N + \boldsymbol{B}_L)\boldsymbol{c} = (\boldsymbol{L}_N + \boldsymbol{B}_L)(\boldsymbol{\eta}-\bar{\boldsymbol{\eta}}_0 + \boldsymbol{c}). \tag{A4}
$$

Next, we show that the matrix $\boldsymbol{L}_N + \boldsymbol{B}_L$ is nonsingular, when $\kappa_{ij,l} \neq 0$. Under Assumption 2, at least one node in $\bar{\mathcal{G}}$ can obtain the information from leader, then we can conclude that at least one $a_{i0} \neq 0$, $i = 1, 2, \ldots, N$. Without loss of generality, it is assumed that there are exactly two nodes r_1 and r_2 such that $a_{r_1,0} > 0$ and $a_{r_2,0} > 0$. Then, for matrix $\boldsymbol{L}_N + \boldsymbol{B}_L$, $\|\boldsymbol{l}_{ii} + a_{i0}\boldsymbol{\kappa}_{i0}\boldsymbol{\rho}_{i0}^{-1}\| \geqslant \sum_{j=1,j\neq i}^{N}\|\boldsymbol{l}_{ij}\|$ for all $i = 1,\ldots,N$ and the strict inequality holds for $a_{i0} \in \{a_{r_2,0}, a_{r_2,0}\}$, where $\boldsymbol{l}_{ii} + a_{i0}\boldsymbol{\kappa}_{i0}\boldsymbol{\rho}_{i0}^{-1}$ is a diagonal matrix. Additionally, Assumption 2 implies that, for any other node i which does not have direct access to the leader node, there must be a directed path originated from either node r_1 or node r_2. According to [1], $\boldsymbol{L}_N + \boldsymbol{B}_L$ is nonsingular, which implies that inequality (A1) can be obtained from (A4). This completes the proof.

Lemma 2. For adaptive law (18), there exists a compact set

$$
\Omega_{\text{wi}} = \left\{\hat{\boldsymbol{W}}_{i,l} \,|\, \|\hat{\boldsymbol{W}}_{i,l}\| \leqslant \frac{S_{i,l}^*}{\sigma_{i,l}},\ l = 1,2,3\right\}
$$

where $S_{i,l}^*$ and $\sigma_{i,l}$ are positive constants, such that, if $\hat{\boldsymbol{W}}_{i,l}(0) \in \Omega_{\text{wi}}$, then $\hat{\boldsymbol{W}}_{i,l}(t) \in \Omega_{\text{wi}}$, $\forall t \geqslant 0$.

Proof: Consider the Lyapunov function $V_{\text{wi}} = \frac{1}{2}\hat{\boldsymbol{W}}_{i,l}^T\boldsymbol{\Gamma}_{i,l}^{-1}\hat{\boldsymbol{W}}_{i,l}$, whose derivative along (18) is

$$
\begin{aligned}
\dot{V}_{\text{wi}} = -\hat{\boldsymbol{W}}_{i,l}^T\boldsymbol{S}_{i,l}(\boldsymbol{Z}_i)z_{i,l} - \sigma_{i,l}|z_{i,l}|\hat{\boldsymbol{W}}_{i,l}^T\hat{\boldsymbol{W}}_{i,l} &\leqslant S_{i,l}^*|z_{i,l}|\|\hat{\boldsymbol{W}}_{i,l}\| - \sigma_{i,l}|z_{i,l}|\|\hat{\boldsymbol{W}}_{i,l}\|^2\\
&\leqslant -|z_{i,l}|\|\hat{\boldsymbol{W}}_{i,l}\|(\sigma_{i,l}\|\hat{\boldsymbol{W}}_{i,l}\| - S_{i,l}^*).
\end{aligned}
$$

It can be concluded that if $\|\hat{\boldsymbol{W}}_{i,l}\| > \frac{S_{i,l}^*}{\sigma_{i,l}}$ then $\dot{V}_{\text{wi}} \leqslant 0$. Thus, $\hat{\boldsymbol{W}}_{i,l}(t) \in \Omega_{\text{wi}}$ holds if $\hat{\boldsymbol{W}}_{i,l}(0) \in \Omega_{\text{wi}}$. This completes the proof.

Now, we are ready to prove Theorem 1. Consider the Lyapunov function candidate

$$
V_1 = \frac{1}{4}\sum_{i=1}^{N}\boldsymbol{s}_i^T\boldsymbol{s}_i
$$

whose derivative along (1) and (9)–(11) is

$$
\dot{V}_1 = \sum_{i=1}^{N}\boldsymbol{s}_i^T[\boldsymbol{E}_i^T(\boldsymbol{F}_i\boldsymbol{J}(\psi_i)(\boldsymbol{z}_i + \boldsymbol{\alpha}_i + \boldsymbol{e}_{\alpha i}) - \boldsymbol{\Pi}_i\boldsymbol{\rho}_i^{-1}\boldsymbol{Q}_i)]. \tag{A5}
$$

Substituting (12) into (A5) gives

$$
\dot{V}_1 = \sum_{i=1}^{N} -\boldsymbol{s}_i^T\boldsymbol{k}_{1i}\boldsymbol{s}_i + \boldsymbol{s}_i^T\boldsymbol{E}_i^T\boldsymbol{F}_i\boldsymbol{J}(\psi_i)(\boldsymbol{e}_{\alpha i} + \boldsymbol{z}_i). \tag{A6}
$$

Using (13), the derivative of (11) is given by

$$
\dot{\boldsymbol{e}}_{\alpha i} = -\boldsymbol{\mu}_i^{-1}\boldsymbol{e}_{\alpha i} - \boldsymbol{J}^T(\psi_i)\boldsymbol{F}_i^T\boldsymbol{E}_i\boldsymbol{s}_i - \boldsymbol{B}_i(\cdot) \tag{A7}
$$

where $\boldsymbol{B}_i(\cdot) = [B_{1i}(\cdot), B_{2i}(\cdot), B_{3i}(\cdot)]^T \triangleq \dot{\boldsymbol{\alpha}}_i$ with $B_{1i}(\boldsymbol{\eta}_0, \dot{\boldsymbol{\eta}}_0, \ddot{\boldsymbol{\eta}}_0, \boldsymbol{\rho}_i, \dot{\boldsymbol{\rho}}_i, \ddot{\boldsymbol{\rho}}_i, \boldsymbol{s}_i, \boldsymbol{z}_i, \boldsymbol{e}_{\alpha i})$, $B_{2i}(\boldsymbol{\eta}_0, \dot{\boldsymbol{\eta}}_0, \ddot{\boldsymbol{\eta}}_0, \boldsymbol{\rho}_i, \dot{\boldsymbol{\rho}}_i, \ddot{\boldsymbol{\rho}}_i, \boldsymbol{s}_i, \boldsymbol{z}_i, \boldsymbol{e}_{\alpha i})$, and $B_{3i}(\boldsymbol{\eta}_0, \dot{\boldsymbol{\eta}}_0, \ddot{\boldsymbol{\eta}}_0, \boldsymbol{\rho}_i, \dot{\boldsymbol{\rho}}_i, \ddot{\boldsymbol{\rho}}_i, \boldsymbol{s}_i, \boldsymbol{z}_i, \boldsymbol{e}_{\alpha i})$ being continuous functions according to (12).

Consider the Lyapunov function candidate

$$
V_2 = V_1 + \frac{1}{2}\sum_{i=1}^{N}\boldsymbol{e}_{\alpha i}^T\boldsymbol{e}_{\alpha i} + \frac{1}{2}\sum_{i=1}^{N}\boldsymbol{z}_i^T\boldsymbol{M}\boldsymbol{z}_i
$$

whose time derivative along systems (A6), (A7) and (14) is given by

$$
\dot{V}_2 = \sum_{i=1}^{N}[-\boldsymbol{s}_i^T\boldsymbol{k}_{1i}\boldsymbol{s}_i + \boldsymbol{s}_i^T\boldsymbol{E}_i^T\boldsymbol{F}_i\boldsymbol{J}(\psi_i)\boldsymbol{z}_i - \boldsymbol{e}_{\alpha i}^T\boldsymbol{\mu}_i^{-1}\boldsymbol{e}_{\alpha i} - \boldsymbol{e}_{\alpha i}^T\boldsymbol{B}_i(\cdot) + \boldsymbol{z}_i^T(-\boldsymbol{\Phi}_i\boldsymbol{m} - \boldsymbol{D}(\boldsymbol{\nu}_i)\boldsymbol{\nu}_i + \boldsymbol{d}_i + \boldsymbol{\tau}_i)] \tag{A8}
$$

where

$$\begin{aligned}\boldsymbol{\Phi}_i\boldsymbol{m} &= \boldsymbol{C}(\boldsymbol{\nu}_i)\boldsymbol{\nu}_i - \boldsymbol{M}(\boldsymbol{\mu}_i^{-1}\boldsymbol{e}_{\alpha i} + \boldsymbol{J}^T(\psi_i)\boldsymbol{F}_i^T\boldsymbol{E}_i\boldsymbol{s}_i)\\ \boldsymbol{m} &= [m_{11}, m_{22}, m_{23}, m_{33}]^T\\ \boldsymbol{\Phi}_i &= \begin{bmatrix}\Phi_{i,11} & -v_ir_i & -r_i^2 & 0\\ u_ir_i & \Phi_{i,22} & \Phi_{i,23} & 0\\ -u_iv_i & v_iu_i & \Phi_{i,33} & \Phi_{i,34}\end{bmatrix}\end{aligned}$$

with $\Phi_{i,11} = -\pi_{ij,1}\rho_{ij,1}^{-1}e_{ij,1}^3\cos\psi_i - \pi_{ij,2}\rho_{ij,2}^{-1}e_{ij,2}^3\sin\psi_i - \frac{e_{\alpha i,1}}{\mu_{i,1}}$, $\Phi_{i,22} = \pi_{ij,1}\rho_{ij,1}^{-1}e_{ij,1}^3\sin\psi_i - \pi_{ij,2}\rho_{ij,2}^{-1}e_{ij,2}^3\cos\psi_i - \frac{e_{\alpha i,2}}{\mu_{i,2}}$, $\Phi_{i,23} = \Phi_{i,34} = -\frac{e_{\alpha i,3}}{\mu_{i,3}} - \pi_{ij,3}\rho_{ij,3}^{-1}e_{ij,3}^3$, $\Phi_{i,33} = r_iu_i + \Phi_{i,22}$.

Note that the uncertain dynamics $\boldsymbol{D}(\boldsymbol{\nu}_i)\boldsymbol{\nu}_i$ is approximated by the Gaussian radial basis function (RBF) NNs. Let

$$f_i(\boldsymbol{Z}_i) = \boldsymbol{D}(\boldsymbol{\nu}_i)\boldsymbol{\nu}_i \tag{A9}$$

where $f_i(\boldsymbol{Z}_i) = [f_{i,1}(\boldsymbol{Z}_i), f_{i,2}(\boldsymbol{Z}_i), f_{i,3}(\boldsymbol{Z}_i)]^T$ and $\boldsymbol{Z}_i = \boldsymbol{\nu}_i = [u_i, v_i, r_i]^T$. Using universal approximation of RBF NNs [2], the unknown continuous functions $f_{i,l}(\boldsymbol{Z}_i)$ can be approximated by

$$f_{i,l}(\boldsymbol{Z}_i) = \boldsymbol{W}_{i,l}^{*T}\boldsymbol{S}_{i,l}(\boldsymbol{Z}_i) + \epsilon_{i,l}(\boldsymbol{Z}_i), \forall \boldsymbol{Z}_i \in \Omega_{zi}$$

with $l = 1, 2, 3$, where $\boldsymbol{W}_{i,l}^*$ denote the ideal constant weights, which are unknown vectors; $\boldsymbol{S}_{i,l}$ are the regressor vectors satisfying $\|\boldsymbol{S}_{i,l}\| \leqslant S_{i,l}^*$ with constants $S_{i,l}^* > 0$; Ω_{zi} denote known compact sets; $\epsilon_{i,l}(\boldsymbol{Z}_i)$ are the approximation errors satisfying $|\epsilon_{i,l}(\boldsymbol{Z}_i)| < \epsilon_{i,l}^*$ with constants $\epsilon_{i,l}^* > 0$. Let $\hat{\boldsymbol{W}}_i^T\boldsymbol{S}_i(\boldsymbol{Z}_i)$ be the approximation of unknown continuous function $f_i(\boldsymbol{Z}_i)$, where $\boldsymbol{S}_i(\boldsymbol{Z}_i) = [\boldsymbol{S}_{i,1}^T(\boldsymbol{Z}_i), \boldsymbol{S}_{i,2}^T(\boldsymbol{Z}_i), \boldsymbol{S}_{i,3}^T(\boldsymbol{Z}_i)]^T$, and $\hat{\boldsymbol{W}}_i^T = \mathrm{diag}[\hat{\boldsymbol{W}}_{i,1}^T, \hat{\boldsymbol{W}}_{i,2}^T, \hat{\boldsymbol{W}}_{i,3}^T]$ are the estimates of the unknown vectors $\boldsymbol{W}_i^{*T} = \mathrm{diag}[\boldsymbol{W}_{i,1}^{*T}, \boldsymbol{W}_{i,2}^{*T}, \boldsymbol{W}_{i,3}^{*T}]$ with estimate errors $\tilde{\boldsymbol{W}}_{i,l} = \hat{\boldsymbol{W}}_{i,l} - \boldsymbol{W}_{i,l}^*$. Note that the time-varying disturbance $\boldsymbol{d}_i$ in (A8) is bounded by unknown positive constant according to Assumption 3. Thus, the disturbances $d_{i,l}$ are compensated by estimating theirs upper bounds.

We have shown in Lemma 2 that $\hat{\boldsymbol{W}}_{i,l}(t)$ are bounded as long as the initial values are chosen appropriately (e.g., $\hat{\boldsymbol{W}}_{i,l}(0) = 0$). Thus, we consider the following Lyapunov function candidate

$$V = V_2 + \frac{1}{2}\sum_{i=1}^N \tilde{\boldsymbol{m}}_i^T\boldsymbol{\Gamma}_m^{-1}\tilde{\boldsymbol{m}}_i + \sum_{i=1}^N\sum_{l=1}^3 \frac{1}{2\gamma_{di,l}}\tilde{\bar{d}}_{i,l}^2 \tag{A10}$$

where $\tilde{\boldsymbol{m}}_i = \hat{\boldsymbol{m}}_i - \boldsymbol{m}$ and $\tilde{\bar{d}}_{i,l} = \hat{\bar{d}}_{i,l} - \bar{d}_{i,l}$. Using (A8) and (16), the derivative of (A10) is

$$\begin{aligned}\dot{V} &= \sum_{i=1}^N[-\boldsymbol{s}_i^T\boldsymbol{k}_{1i}\boldsymbol{s}_i - \boldsymbol{e}_{\alpha i}^T\boldsymbol{\mu}_i^{-1}\boldsymbol{e}_{\alpha i} - \boldsymbol{z}_i^T\boldsymbol{k}_{2i}\boldsymbol{z}_i + \boldsymbol{z}_i^T\boldsymbol{\Phi}_i\tilde{\boldsymbol{m}}_i + \boldsymbol{z}_i^T\tilde{\boldsymbol{W}}_i^T\boldsymbol{S}_i(\boldsymbol{Z}_i) - \boldsymbol{z}_i^T\boldsymbol{\epsilon}_i(\boldsymbol{Z}_i) - \boldsymbol{e}_{\alpha i}^T\boldsymbol{B}_i(\cdot)\\ &\quad +\tilde{\boldsymbol{m}}_i^T\boldsymbol{\Gamma}_m^{-1}\dot{\tilde{\boldsymbol{m}}}_i + \sum_{l=1}^3(\frac{1}{\gamma_{di,l}}\tilde{\bar{d}}_{i,l}\dot{\hat{\bar{d}}}_{i,l} + z_{i,l}d_{i,l} - z_{i,l}\hat{\bar{d}}_{i,l}\tanh(\frac{z_{i,l}\hat{\bar{d}}_{i,l}}{\zeta}))]\end{aligned} \tag{A11}$$

where $\boldsymbol{\epsilon}_i(\boldsymbol{Z}_i) = [\epsilon_{i,1}(\boldsymbol{Z}_i), \epsilon_{i,2}(\boldsymbol{Z}_i), \epsilon_{i,3}(\boldsymbol{Z}_i)]^T$. Substituting (17) and (19) into (A11) yields

$$\begin{aligned}\dot{V} &= \sum_{i=1}^N[-\boldsymbol{s}_i^T\boldsymbol{k}_{1i}\boldsymbol{s}_i - \boldsymbol{e}_{\alpha i}^T\boldsymbol{\mu}_i^{-1}\boldsymbol{e}_{\alpha i} - \boldsymbol{z}_i^T\boldsymbol{k}_{2i}\boldsymbol{z}_i + \boldsymbol{z}_i^T\tilde{\boldsymbol{W}}_i^T\boldsymbol{S}_i(\boldsymbol{Z}_i) - \boldsymbol{z}_i^T\boldsymbol{\epsilon}_i(\boldsymbol{Z}_i) - \boldsymbol{e}_{\alpha i}^T\boldsymbol{B}_i(\cdot) - \sigma_m\tilde{\boldsymbol{m}}_i^T\hat{\boldsymbol{m}}_i\\ &\quad -\beta_m\tilde{\boldsymbol{m}}_i^T\boldsymbol{\Psi}_{m,i} + \sum_{l=1}^3(-\sigma_{di,l}\tilde{\bar{d}}_{i,l}\hat{\bar{d}}_{i,l} + z_{i,l}d_{i,l} - |z_{i,l}|\bar{d}_{i,l}) + \sum_{l=1}^3(|z_{i,l}|\hat{\bar{d}}_{i,l} - z_{i,l}\hat{\bar{d}}_{i,l}\tanh(\frac{z_{i,l}\hat{\bar{d}}_{i,l}}{\zeta}))]\end{aligned} \tag{A12}$$

where

$$\sum_{i=1}^N \beta_m\tilde{\boldsymbol{m}}_i^T\boldsymbol{\Psi}_{m,i} = \beta_m\tilde{\boldsymbol{m}}^T(\mathcal{L}\otimes I_4)\tilde{\boldsymbol{m}} \tag{A13}$$

with $\tilde{\boldsymbol{m}} = [\tilde{\boldsymbol{m}}_1^T, \ldots, \tilde{\boldsymbol{m}}_N^T]^T$, $\mathcal{L}$ being the Laplacian matrix of graph $\mathcal{G}$, and the operator $\otimes$ being the kronecker product. From Assumption 3, we know that $z_{i,l}d_{i,l} \leqslant |z_{i,l}|\bar{d}_{i,l}$. Noting the property of $\tanh(\cdot)$ [3, Lemma 5], i.e., the following inequality

$$0 \leqslant |a| - a\tanh(\frac{a}{\zeta}) \leqslant \kappa_p\zeta,\ \kappa_p = 0.2785$$

holds for all $\zeta > 0$ and $a \in \Re$. Combining the fact that $|z_{i,l}|\hat{\bar{d}}_{i,l} \leqslant |z_{i,l}||\hat{\bar{d}}_{i,l}|$, we have

$$|z_{i,l}|\hat{\bar{d}}_{i,l} - z_{i,l}\hat{\bar{d}}_{i,l}\tanh(\frac{z_{i,l}\hat{\bar{d}}_{i,l}}{\zeta}) \leqslant \kappa_p\zeta. \tag{A14}$$

It follows from Lemma 2 that $\hat{\boldsymbol{W}}_{i,l}$ is bounded when the design initial condition satisfies $\hat{\boldsymbol{W}}_{i,l}(0) \in \Omega_{\mathrm{wi}}$. Then, the NN weight estimate error $\tilde{\boldsymbol{W}}_{i,l}$ is also bounded using $\tilde{\boldsymbol{W}}_{i,l} = \hat{\boldsymbol{W}}_{i,l} - \boldsymbol{W}_{i,l}^*$ and the boundedness of $\boldsymbol{W}_{i,l}^*$. Therefore, there exists a positive constant $\bar{w}_{i,l}$ such that $\|\tilde{\boldsymbol{W}}_{i,l}\| < \bar{w}_{i,l}$. Noting the property of the Gaussian radial basis function that $\boldsymbol{S}_{i,l}(\boldsymbol{Z}_i)$ satisfies $\|\boldsymbol{S}_{i,l}(\boldsymbol{Z}_i)\| \leqslant S_{i,l}^*$ with constant $S_{i,l}^* > 0$. By completion of squares, we have

$$\boldsymbol{z}_i^T\tilde{\boldsymbol{W}}_i^T\boldsymbol{S}_i(\boldsymbol{Z}_i) \leqslant \frac{\kappa_i}{2}\|\boldsymbol{z}_i\|^2 + \sum_{l=1}^3\frac{3\bar{w}_{i,l}^2S_{i,l}^{*2}}{2\kappa_i},\quad -\boldsymbol{z}_i^T\boldsymbol{\epsilon}_i(\boldsymbol{Z}_i) \leqslant \frac{\kappa_i}{2}\|\boldsymbol{z}_i\|^2 + \sum_{l=1}^3\frac{\epsilon_{i,l}^{*2}}{2\kappa_i}$$

$$-\sigma_m\tilde{\boldsymbol{m}}_i\hat{\boldsymbol{m}}_i \leqslant -\frac{1}{2}\sigma_m\tilde{\boldsymbol{m}}_i^T\tilde{\boldsymbol{m}}_i + \frac{1}{2}\sigma_m\|\boldsymbol{m}\|^2, \quad -\sigma_{di,l}\tilde{\bar{d}}_{i,l}\hat{\bar{d}}_{i,l} \leqslant -\frac{1}{2}\sigma_{di,l}\tilde{\bar{d}}_{i,l}^2 + \frac{1}{2}\sigma_{di,l}\bar{d}_{i,l}^2 \tag{A15}$$

where $\kappa_i > 0$ is a design parameter. Consider the sets $\mathcal{O}_1 := \{\sum_{i=1}^N(\|\boldsymbol{s}_i\|^2 + \|\boldsymbol{z}_i\|^2 + \|\boldsymbol{e}_{\alpha,i}\|^2 + \|\tilde{\boldsymbol{m}}_i\|^2 + \|\tilde{\bar{\boldsymbol{d}}}_i\|^2) \leqslant 2\varsigma\}$ and $\mathcal{O}_2 := \{\|\bar{\boldsymbol{\eta}}_0\|^2 + \|\dot{\bar{\boldsymbol{\eta}}}_0\|^2 + \|\ddot{\bar{\boldsymbol{\eta}}}_0\|^2 + \sum_{i=1}^N(\|\boldsymbol{\rho}_i\|^2 + \|\dot{\boldsymbol{\rho}}_i\|^2 + \|\ddot{\boldsymbol{\rho}}_i\|^2) \leqslant B_d\}$ with constants $\varsigma > 0$ and $B_d > 0$. Using the continuous property and equation (A7), we have that the continuous function $\boldsymbol{B}_i(\cdot)$ is bounded on the compact set $\mathcal{O}_1 \times \mathcal{O}_2$. Thus, there exists a positive constant $\bar{B}_i$ such that $\|\boldsymbol{B}_i(\cdot)\| \leqslant \bar{B}_i$ on $\mathcal{O}_1 \times \mathcal{O}_2$. Then, we have

$$-\boldsymbol{e}_{\alpha i}^T\boldsymbol{B}_i(\cdot) \leqslant \frac{\kappa_i}{2}\|\boldsymbol{e}_{\alpha i}\|^2 + \frac{\bar{B}_i^2}{2\kappa_i}. \tag{A16}$$

Substituting (A13)–(A16) into (A12) yields

$$\begin{aligned}\dot{V} \leqslant & \sum_{i=1}^N[-\boldsymbol{s}_i^T\boldsymbol{k}_{1i}\boldsymbol{s}_i - \boldsymbol{e}_{\alpha i}^T(\boldsymbol{\mu}_i^{-1} - \frac{\kappa_i I_3}{2})\boldsymbol{e}_{\alpha i} - \boldsymbol{z}_i^T(\boldsymbol{k}_{2i} - \kappa_i I_3)\boldsymbol{z}_i - \sum_{l=1}^3\frac{\sigma_{di,l}}{2}\tilde{\bar{d}}_{i,l}^2] - \tilde{\boldsymbol{m}}^T\mathcal{L}_m\tilde{\boldsymbol{m}} \\ & + \sum_{i=1}^N[\sum_{l=1}^3(\frac{\sigma_{di,l}}{2}\bar{d}_{i,l}^2 + \frac{\epsilon_{i,l}^{*2} + 3\bar{w}_{i,l}^2S_{i,l}^{*2}}{2\kappa_i}) + \frac{\sigma_m}{2}\|\boldsymbol{m}\|^2 + \frac{\bar{B}_i^2}{2\kappa_i}] + 3\kappa_p\zeta N\end{aligned} \tag{A17}$$

where $\mathcal{L}_m = 0.5\sigma_m I_{4N} + \beta_m\mathcal{L}\otimes I_4$ and the design parameters σ_m and β_m are chosen such that the matrix $\mathcal{L}_m$ is positive definite. Note that equation (A10) can be rewritten as

$$V = \frac{1}{4}\sum_{i=1}^N\boldsymbol{s}_i^T\boldsymbol{s}_i + \frac{1}{2}\sum_{i=1}^N\boldsymbol{e}_{\alpha i}^T\boldsymbol{e}_{\alpha i} + \frac{1}{2}\sum_{i=1}^N\boldsymbol{z}_i^T\boldsymbol{M}\boldsymbol{z}_i + \sum_{i=1}^N\sum_{l=1}^3\frac{1}{2\gamma_{di,l}}\tilde{\bar{d}}_{i,l}^2 + \frac{1}{2}\sum_{i=1}^N\tilde{\boldsymbol{m}}_i^T\boldsymbol{\Gamma}_m^{-1}\tilde{\boldsymbol{m}}_i. \tag{A18}$$

Using (A18) and (A17), we can obtain

$$\dot{V} \leqslant -\varrho V + \delta \tag{A19}$$

where

$$\begin{aligned}\varrho &= \min\Big\{4\boldsymbol{k}_{1i}, 2\boldsymbol{\mu}_i^{-1} - \kappa_i I_3, \frac{2\lambda_{\min}(\boldsymbol{k}_{2i} - \kappa_i I_3)}{\lambda_{\max}(\boldsymbol{M})}, \sigma_{di,l}\gamma_{di,l}, \frac{2\lambda_{\min}(\mathcal{L}_m)}{\lambda_{\max}(\boldsymbol{\Gamma}_m^{-1})}\Big\} \\ \delta &= \sum_{i=1}^N\sum_{l=1}^3\frac{\sigma_{di,l}\kappa_i\bar{d}_{i,l}^2 + \epsilon_{i,l}^{*2} + 3\bar{w}_{i,l}^2S_{i,l}^{*2}}{2\kappa_i} + \sum_{i=1}^N\frac{\sigma_m\kappa_i\|\boldsymbol{m}\|^2 + \bar{B}_i^2}{2\kappa_i} + 3\kappa_p\zeta N\end{aligned} \tag{A20}$$

where $\lambda_{\min}(\cdot)$ and $\lambda_{\max}(\cdot)$ denote the minimum and maximum eigenvalue of the corresponding matrix, respectively. For choosing $\varrho > \delta/\varsigma$, we have $\dot{V} \leqslant 0$ on $V = \varsigma$. Therefore, $V \leqslant \varsigma$ is an invariant set, i.e., if $V(0) \leqslant \varsigma$, then $V(t) \leqslant \varsigma$ for all $t > 0$. Inequality (A19) implies that

$$V(t) \leqslant (V(0) - \delta/\varrho)\exp(-\varrho t) + \delta/\varrho, \quad \forall t \geqslant 0 \tag{A21}$$

which indicates that $V(t)$ is bounded. Then, the local neighborhood transformed errors $\boldsymbol{s}_i$ are bounded. As time tends to infinity, $\boldsymbol{s} = [\boldsymbol{s}_1^T, \boldsymbol{s}_2^T, \ldots, \boldsymbol{s}_N^T]^T$ converges exponentially to the set $\Omega = \{\boldsymbol{s}|\|\boldsymbol{s}\| \leqslant 4\sqrt{\delta/\varrho}\}$, whose size can be adjusted by tuning the design parameters. Using Lemma 1, we have

$$\lim_{t\to\infty}\|\boldsymbol{\eta} - \bar{\boldsymbol{\eta}}_0 + \boldsymbol{c}\| \leqslant \frac{4\sqrt{\delta/\varrho}}{\sigma_{\min}(\boldsymbol{L}_N + \boldsymbol{B}_L)}$$

which indicates that the inequality $\lim_{t\to\infty}\|\boldsymbol{\eta}_i - \boldsymbol{\eta}_0 + \boldsymbol{c}_i\| < \varepsilon$ holds and the positive constant ε can be made sufficiently small by choosing appropriate design parameters. Then, we have $\lim_{t\to\infty}\|\dot{\boldsymbol{\eta}}_i - \dot{\boldsymbol{\eta}}_0\| < \bar{\varepsilon}$ with $\bar{\varepsilon}$ being constant, which means that the velocities of each vehicle converge to a small neighbourhood around the leader's velocities.

It follows from (A21) that $\boldsymbol{s}_i = \sum_{j\in\mathcal{N}_i}a_{ij}\boldsymbol{q}_{ij} + a_{i0}\boldsymbol{q}_{i0}$ are bounded. Invoking $\boldsymbol{q}_{ij} = [e_{ij,1}^2, e_{ij,2}^2, e_{ij,3}^2]^T$, we know that $e_{ij,l}$ are bounded with $i = 1,\ldots,N$, $l = 1,2,3$, $j \in \mathcal{N}_i$. Subsequently, the inequalities $-1 < p_{ij,l}/\rho_{ij,l} < 1$ hold using equation (4) and the boundedness of $e_{ij,l}$. Then, we have $|p_{ij,l}| < \rho_{ij,l}$ due to $\rho_{ij,l} > 0$. Using (3) and (5), we obtain that $|x_i - x_j| < \frac{\bar{L}_i}{\sqrt{2}}$, $|y_i - y_j| < \frac{\bar{L}_i}{\sqrt{2}}$, and $|\psi_i - \psi_j| < \frac{\pi}{2}$. Thus, if $\|\boldsymbol{\eta}_{i,L}(0) - \boldsymbol{\eta}_{j,L}(0)\| < \bar{L}_i$, $j \in \mathcal{N}_i(0)$, then $\|\boldsymbol{\eta}_{i,L}(t) - \boldsymbol{\eta}_{j,L}(t)\| < \bar{L}_i$ for all $t \geqslant 0$, that is, the connectivity preservation among the initial connected USVs can be guaranteed. This completes the proof.

Appendix B Simulation Studies

To demonstrate the effectiveness of the proposed synchronization tracking control algorithm, we conduct numerical simulation on a group of four identical USVs ($N = 4$) whose dynamics are described by system (1). The vehicle parameters are borrowed from [4], where all quantities are expressed in the international system of units (SI). The matrices in (1) are given by

$$\boldsymbol{J}(\psi_i) = \begin{bmatrix}\cos\psi_i & -\sin\psi_i & 0\\ \sin\psi_i & \cos\psi_i & 0\\ 0 & 0 & 1\end{bmatrix},\ \boldsymbol{M} = \begin{bmatrix}m_{11} & 0 & 0\\ 0 & m_{22} & m_{23}\\ 0 & m_{23} & m_{33}\end{bmatrix},\ \boldsymbol{C}(\boldsymbol{\nu}_i) = \begin{bmatrix}0 & 0 & c_{13}\\ 0 & 0 & c_{23}\\ -c_{13} & -c_{23} & 0\end{bmatrix},\ \boldsymbol{D}(\boldsymbol{\nu}_i) = \begin{bmatrix}d_{11} & 0 & 0\\ 0 & d_{22} & d_{23}\\ 0 & d_{32} & d_{33}\end{bmatrix}$$

where $m_{33} = 2.76$, $m_{23} = 1.0948$, $m_{22} = 33.8$, $m_{11} = 25.8$, $c_{13}(v_i, r_i) = -m_{22}v_i - m_{23}r_i$, $c_{23}(u_i) = m_{11}u_i$, $d_{11}(u_i) = 0.7225 + 1.3274|u_i| + 5.8664u_i^2$, $d_{22}(v_i, r_i) = 0.8612 + 36.2823|v_i| + 0.805|r_i|$, $d_{23}(v_i, r_i) = -0.1079 + 0.845|v_i| + 3.45|r_i|$, $d_{32}(v_i, r_i) = -0.1052 - 5.0437|v_i| - 0.13|r_i|$, $d_{33}(v_i, r_i) = 1.9 - 0.08|v_i| + 0.75|r_i|$. Without loss of generality, the external time-varying disturbances satisfying Assumption 3 are chosen as $\boldsymbol{d}_i = [2 + 4\sin(0.1t), -3 + 2\cos(0.08t), 2 - 0.5\sin(0.05t)]^T$, which is borrowed from section 7.5 in the work of [5]. The choice of such disturbances indicates there exist both constant bias and time-varying external disturbances that act on surge, sway, and yaw dynamics of the vehicle. It should be pointed out that the system parameters including the vehicle inertia and the hydrodynamic damping terms, and the external disturbances are unknown to the control inputs $\boldsymbol{\tau}_i$.

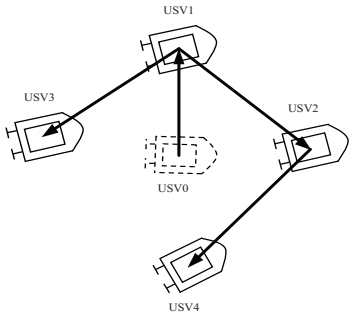

Figure B1 The initial communication topology with geometry shape among one leader and four followers.

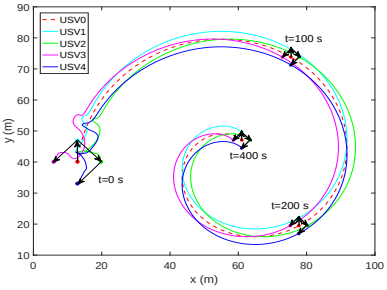

Figure B2 The phase-plane trajectories of vehicle j ($j = 0, 1, \ldots, 4$) and their snapshots at several key times.

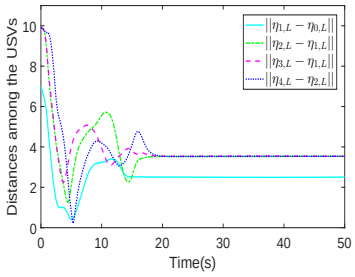

Figure B3 The distances among the initial connected USVs.

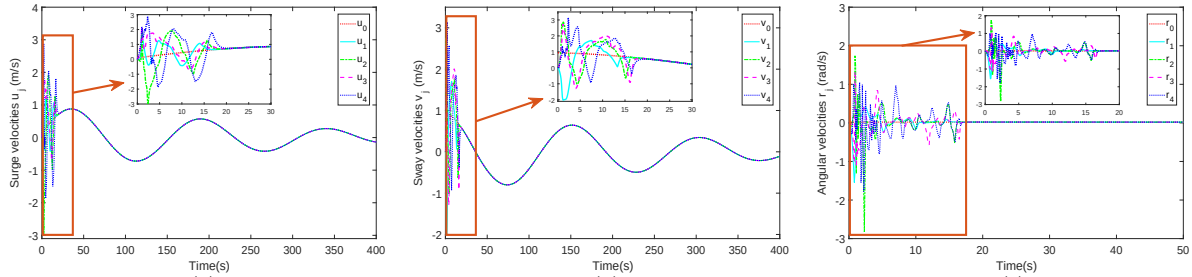

Figure B4 Convergence of the vehicles' velocities. (a) Surge velocities u_j. (b) Sway velocities v_j. (c) Angular velocities r_j.

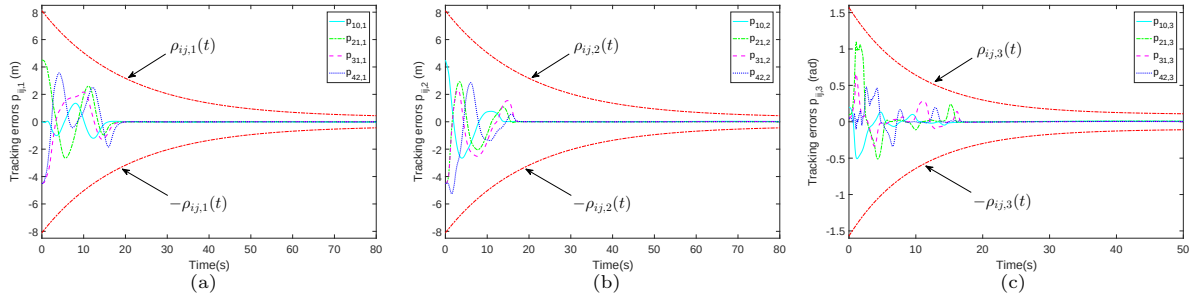

Figure B5 Evolution of the synchronization tracking errors along with the performance functions $\rho_{ij,l}(t)$ and $-\rho_{ij,l}(t)$. (a) $p_{ij,1}(t)$. (b) $p_{ij,2}(t)$. (c) $p_{ij,3}(t)$.

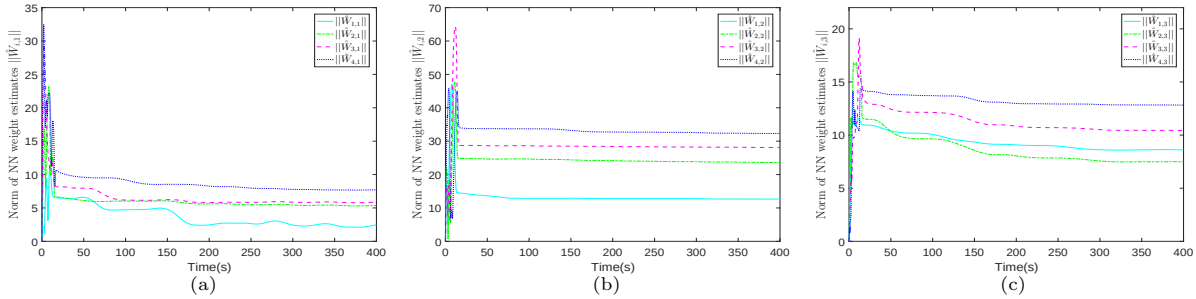

Figure B6 2-norm of NN weight estimates $\|\hat{\boldsymbol{W}}_{i,l}\|$. (a) $\|\hat{\boldsymbol{W}}_{i,1}\|$. (b) $\|\hat{\boldsymbol{W}}_{i,2}\|$. (c) $\|\hat{\boldsymbol{W}}_{i,3}\|$.

The virtual leader's trajectory is given by $\boldsymbol{\eta}_0 = [60 - (15\pi - 0.1t)\cos(wt), 40 + (15\pi - 0.1t)\sin(wt), wt]^T$ which is a spiral curve with $w = 0.02$. Assume the allowed maximal communication radii are $\bar{L}_i = 15$ $(i = 1, \ldots, 4)$, the desired offsets are $\boldsymbol{c}_0 = [0, 0, 0]^T$, $\boldsymbol{c}_1 = [0, -2.5, 0]^T$, $\boldsymbol{c}_2 = [-2.5, 0, 0]^T$, $\boldsymbol{c}_3 = [2.5, 0, 0]^T$, $\boldsymbol{c}_4 = [0, 2.5, 0]^T$. The initial communication topology with geometry shape of the multi-vehicle system is given in Fig. B1, where the neighboring sets are $\mathcal{N}_1 = \{0\}$, $\mathcal{N}_2 = \{1\}$, $\mathcal{N}_3 = \{1\}$, $\mathcal{N}_4 = \{2\}$. Subsequently, the relative desired offsets of neighbors are obtained by $\boldsymbol{c}_{10} = [0, -2.5, 0]^T$, $\boldsymbol{c}_{21} = [-2.5, 2.5, 0]^T$, $\boldsymbol{c}_{31} = [2.5, 2.5, 0]^T$, and $\boldsymbol{c}_{42} = [2.5, 2.5, 0]^T$.

Note that the uncertain dynamics in (A9) can be rewritten as $f_i(\boldsymbol{Z}_i) = [f_{i,1}(u_i), f_{i,2}(v_i, r_i), f_{i,3}(v_i, r_i)]^T$. Then, the Gaussian

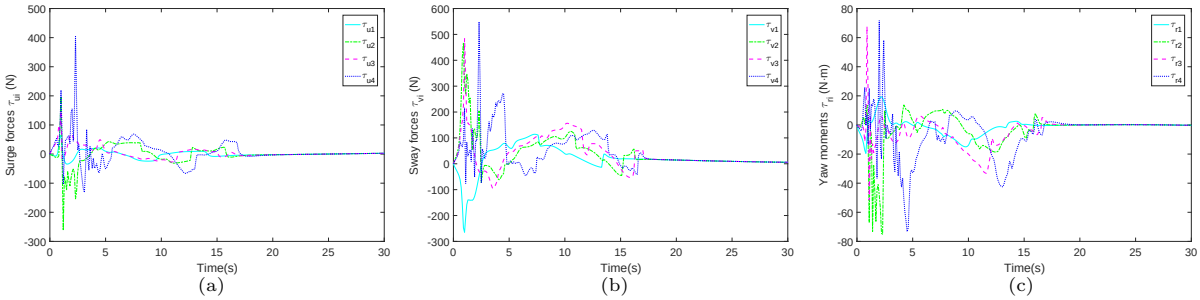

Figure B7 Control inputs $\boldsymbol{\tau}_i$. (a) Surge forces τ_{ui}. (b) Sway forces τ_{vi}. (c) Yaw moments τ_{ri}.

RBF NNs $\hat{\boldsymbol{W}}_{i,1}^T S_{i,1}(u_i)$ are constructed by 20 nodes with the centers of nodes being linearly spaced on $[-2, 2]$ and the widths being 1. Similarly, the Gaussian RBF NNs $\hat{\boldsymbol{W}}_{i,2}^T S_{i,2}(v_i, r_i)$ and $\hat{\boldsymbol{W}}_{i,3}^T S_{i,3}(v_i, r_i)$ are constructed by 20 nodes with the centers of nodes being linearly spaced on $[-2, 2] \times [-0.5, 0.5]$ and the widths being 1, respectively. The design parameters for the NN update law (18) are chosen as $\boldsymbol{\Gamma}_{i,l} = 2$ and $\sigma_{i,l} = 0.01$ with $l = 1, 2, 3$. The design parameters for the performance functions in (5) are chosen as $\rho_{ij,1,0} = \rho_{ij,2,0} = \frac{15}{\sqrt{2}} - 2.5$, $\rho_{ij,3,0} = \frac{\pi}{2}$, $\rho_{i,j,1,\infty} = \rho_{i,j,2,\infty} = 0.3$, $\rho_{i,j,3,\infty} = 0.1$, $k_{i,j,1} = k_{i,j,2} = 0.05$, $k_{i,j,3} = 0.1$, $i = 1, \ldots, 4$, $j \in \mathcal{N}_i$. Other design parameters are taken as $\boldsymbol{k}_{11} = \boldsymbol{k}_{12} = \mathrm{diag}[0.5, 1, 3]$, $\boldsymbol{k}_{13} = \boldsymbol{k}_{14} = \mathrm{diag}[0.5, 1, 4]$, $\boldsymbol{k}_{21} = \boldsymbol{k}_{22} = \boldsymbol{k}_{23} = \mathrm{diag}[1, 1, 2]$, $\boldsymbol{k}_{24} = \mathrm{diag}[1, 1, 4]$, $\boldsymbol{\Gamma}_m = \mathrm{diag}[2, 2, 2, 2]$, $\sigma_m = 0.1$, $\beta_m = 0.01$, $\gamma_{di,l} = 1$, $\sigma_{di,l} = 0$, $\zeta = 1$, $\boldsymbol{\mu}_i = \mathrm{diag}[0.05, 0.05, 0.05]$, $l = 1, 2, 3$. The initial states of the vehicles are $\boldsymbol{\eta}_0(0) = [60 - 15\pi, 40, 0]^T$, $\boldsymbol{\eta}_1(0) = [60 - 15\pi, 47, 0.2]^T$, $\boldsymbol{\eta}_2(0) = [67 - 15\pi, 40, 0.3]^T$, $\boldsymbol{\eta}_3(0) = [53 - 15\pi, 40, 0.25]^T$, $\boldsymbol{\eta}_4(0) = [60 - 15\pi, 33, 0.35]^T$, and $\boldsymbol{\nu}_i(0) = [0, 0, 0]^T$. The initial estimates are chosen as $\hat{\boldsymbol{m}}_i(0) = [0, 0, 0, 0]^T$, $\hat{\bar{\boldsymbol{d}}}_i(0) = [0, 0, 0]^T$, and $\hat{\boldsymbol{W}}_{i,l}(0) = \boldsymbol{0}$.

Simulation results are presented in Figs. B2–B7. Fig. B2 provides the phase-plane trajectories of the vehicle group and their snapshots at 0s, 100s, 200s and 400s, which illustrates that the followers in the vehicle group synchronously tracks the virtual leader while achieving the desired synchronization shape. It follows from Fig. B3 that the distances among the initial connected USVs are preserved always within the allowed communication range, which indicates that the connectivity among the initial connected vehicles is maintained over time. To further demonstrate the synchronization motion of the vehicle group, the velocities of all vehicles including the virtual leader are plotted in Fig. B4. It can be seen from Fig. B4 that the followers' velocities converge to small neighbourhoods around the leader's velocities after transient stage, which indicates that the synchronization motion of the vehicle group is attained after transient stage. Fig. B5 depicts that the synchronization tracking errors $p_{ij,l}$ eventually converge to a small neighborhood of zero without violating the performance requirements specified by the performance function (5), which means that $\boldsymbol{s}_i$ are bounded using (6). It follows that the distances between USVs i and j satisfy (2) for all time, i.e., the initial connectivity among all vehicles are maintained. The 2-norm of NN weight estimates $\|\hat{\boldsymbol{W}}_{i,l}\|$ are presented in Fig. B6, which shows the boundedness of NN weight estimates. Fig. B7 illustrates that the control inputs $\boldsymbol{\tau}_i$ are bounded.

References

1 P. Shivakumar and K. Chew, "A sufficient condition for nonvanishing of determinants," *Proceedings of The American Mathematical Society-PROC AMER MATH SOC*, vol. 43, 1974.

2 S.-L. Dai, C. Wang, and M. Wang, "Dynamic learning from adaptive neural network control of a class of nonaffine nonlinear systems," *IEEE Transactions on Neural Networks and Learning Systems*, vol. 25, no. 1, pp. 111–123, 2014.

3 S.-L. Dai, K. Lu, and X. Jin, "Fixed-time formation control of unicycle-type mobile robots with visibility and performance constraints," *IEEE Transactions on Industrial Electronics*, DOI: 10.1109/TIE.2020.3040686, Early Access Online, 2020.

4 S. He, M. Wang, S.-L. Dai, and F. Luo, "Leader-follower formation control of USVs with prescribed performance and collision avoidance," *IEEE Transactions on Industrial Informatics*, vol. 15, no. 1, pp. 572–581, 2019.

5 K. D. Do and J. Pan, *Control of Ships and Underwater Vehicles: Design for Underactuated and Nonlinear Marine Systems*. Springer Verlag, 2009.